ELSEVIER

Comput. Methods Appl. Mech. Engrg. 129 (1996) 349–370

Computer methods in applied mechanics and engineering

Superconvergent extraction of flux intensity factors and first derivatives from finite element solutions

Barna A. Szabó, Zohar Yosibash *

Center for Computational Mechanics, Washington University, Campus Box 1129, St. Louis, MO 63130, USA

Received 14 September 1994; revised 16 February 1995

Abstract

A superconvergent method for the computation of the derivatives of the solution and the coefficients of the asymptotic expansion at singular points is presented for the Laplace problem in two dimensions. The algorithm utilizes the complementary weak form on a localized small domain. Mathematical analysis demonstrates the superconvergent behavior, and numerical experiments support our analysis. This method is well suited for anisotropic multi-material singular interface problems.

1. Introduction

The problem of quality control in finite element computations has been the subject of many recent investigations. Most of the work has been concerned with estimation and control of error in energy norm (see [1, Chapters 4 and 10] and the references therein). These are *average measures*, however. In most cases, determination of the location and magnitude of the largest first derivative (flux for example in heat transfer problem), or flux intensity factors (in the vicinity of singular points) is of interest. These are *pointwise* quantities.

This paper presents a superconvergent method for the extraction of these quantities from finite element solutions. This is a post-solution operation over a localized small subdomain. The advantages of the new approach over existing ones are due to its generality in the sense that it is applicable to all parts of the solution domain, interior points as well as the boundary points, and also in the neighborhood of singularities. We demonstrate the method on the basis of the two-dimensional Laplace problem. This problem has been chosen because it is simple enough for demonstration purposes, yet contains all essential properties which are common to elliptic boundary value problems. The p-version of the finite element method is employed.

*Corresponding author. Present address: Pearlstone Center for Aeronautical Engineering Studies, Department of Mechanical Engineering, Ben-Gurion University of the Negev, PO Box 653, Beer-Sheva 84105, Israel.

SSDI 0045-7825(95)00865-9

1.1. Flux intensity factors

The behavior of the solution for the Laplace equation ($\nabla^2 u = 0$) in a two-dimensional domain in the vicinity of a singular point is best understood and is given by (see [2–5])

$$u = \sum_{i=1}^{\infty} \sum_{s=0}^{S} \sum_{m=0}^{M} C_{ism} f_{ism}(\theta) r^{\alpha_i + m} \ln^s(r), \tag{1}$$

r and θ being the polar coordinates of a system located in the singular point. α_i are the eigenvalues (real numbers in case of the Laplace problem) and $f_{ism}(\theta)$ are the eigenfunctions which are analytical. Except for special cases, $S = 0$. M is either 0, or a positive integer when the boundary near the singular point (at the vertex) is curved. Note that the eigenpairs are uniquely determined by the geometry and material data.

Methods for the computation of the eigenpairs are presented in [3, 4, 6].

Notice that if $\alpha_i < 1$, the corresponding ith term in the expansion equation (1) for ∇u is unbounded as $r \to 0$. We can think of the coefficients C_{ism} of these terms as analogous to the stress intensity factors of elasticity. We generalize this terminology, and refer to all coefficients C_{ism}, whether or not the corresponding terms in Eq. (1) are singular, as generalized flux intensity factors (GFIFs). The analogous coefficients in elasticity are called generalized stress intensity factors (GSIFs). The GSIFs are very important from the engineering point of view because they are related to failure theories.

Many methods exist for the extraction of stress intensity factors associated with *cracks* from finite element solutions. For example, the J-integral method, the energy release rate method, the stiffness derivative method, the contour integral method (CIM), the cutoff function method (CFM), the singular superelement method, etc. (see [7–10] and references therein). Most of the methods, however, are applicable to crack singularities in isotropic materials only and do not provide any desired number of stress intensity factors.

One of the most efficient ways for extracting the GSIFs in a superconvergent manner is by indirect extraction procedure using the CIM and the CFM presented in [7, 9]. These efficient procedures use specially constructed extraction functions. Assume that a desired functional value $Y(u)$ (for example the ith GFIF) is to be computed from the finite element solution, then an expression which is of the form

$$Y(u_{\mathrm{FE}}) = \mathcal{B}(u_{\mathrm{FE}}, v) + Q(v) \tag{2}$$

is constructed, where v is a suitably chosen test function, called the extraction function, $\mathcal{B}(u_{\mathrm{FE}}, v)$ is the bi-linear form of the finite element method and $Q(v)$ is a given functional. The error in the functional value computed by indirect methods can be written as

$$|Y(u) - Y(u_{\mathrm{FE}})| \leqslant ||u - u_{\mathrm{FE}}||_{H^1(\Omega)} \, ||w - w_{\mathrm{FE}}||_{H^1(\Omega)} \tag{3}$$

where w_{FE} is the finite element solution of an auxiliary problem, the exact solution of which is w. Specifically, w is the projection of v onto the space of admissible functions. In many cases it is possible to select the extraction function v so that $||w - w_{\mathrm{FE}}||_{H^1(\Omega)} \to 0$ not slower, and possibly much faster, than $||u - u_{\mathrm{FE}}||_{H^1(\Omega)} \to 0$ as the number of degrees of freedom approaches infinity, in an orderly extension process. Therefore, functional values computed by these kind of indirect methods have the same order of accuracy as the square of the error measured in the natural norm of the formulation or better. The extraction function for the ith GFIF are chosen to be the eigenfunctions in Eq. (1) which correspond to the negative ith eigenvalue.

These methods have three major drawbacks. First, the CIM is not directly applicable to anisotropic multi-material interfaces[1] because the eigenfunctions are not orthogonal with respect to the bilinear form. Second, a large number of extraction functions must be devised. Third, in the general elliptic

[1] The PDE in an anisotropic domain is given by $\sum_{i,j=1}^{2} a_{ij} \partial^2 u/(\partial x_i \, \partial x_j) = 0$. Laplace's equation is an isotropic case where $a_{11} = a_{22} = 1$, $a_{12} = 0$. A multi-material interface situation is when a_{ij} change abruptly within the domain.

problems these auxiliary functions are considerably less smooth, so that they cannot be approximated by the finite element method as well as the eigenfunctions corresponding to positive eigenvalues.

The method presented in the following has the advantages of these superconvergent methods, without the drawbacks. Numerical examples on the performance of the proposed method for anisotropic domains and multi-material interfaces can be found in [11].

1.2. Extraction of the first derivatives

Typically, first derivatives are extracted from finite element solutions by the direct method. The direct method of extraction is described in detailed in [1, Section 11.4.1]. In the case of elasticity, for example, the strains are computed from the displacement components and the stresses from the appropriate stress–strain law.

The pointwise derivatives extracted by the direct method from the finite element solution do not (in general) converge monotonically (even though the error in energy norm does), and their rate of convergence is usually dependent on the smoothness of the exact solution. In the first element adjacent to a singular point, for example, the derivatives oscillate with high amplitudes as the p-level is increased. Only when the exact solution is relatively smooth do the derivatives extracted by the direct method converge in a satisfactory manner, and their rates of convergence for high p-levels are similar to the error in the energy norm. This behavior is demonstrated in [12]. As the exact solution becomes progressively less smooth, the performance of the direct method deteriorates, and indirect extraction methods should be sought.

Indirect computation of stresses has been shown to be superior to direct methods (see for example [13–16]). The methods presented in [13–15] are based on same idea presented in Eq. (2) so that some measure of artificial intelligence should be applied in general purpose computer programs in the sense that the proper extraction functions must be selected automatically, depending on the problem parameters and the *type* and *location* of output information required. We do not know of any practical implementation of indirect extraction techniques for the derivatives, even though the method has been known for almost ten years. The patch recovery method, in [16], does not perform satisfactorily in the neighborhood of singular points.

The method presented in this paper, on the other hand, is superconvergent, fully general and may be implemented in any finite element code.

The outline of the paper is as follows. The notations and the general formulation and description of the suggested extraction method is followed. In Section 3 we present the weak formulation for the extraction of the GFIFs. A mathematical analysis is presented which demonstrates that the method exhibits superconvergence. Numerical experiments are presented in Section 4 on the basis of two model problems, a crack in a circular domain and an L-shaped domain. We also provide numerical examples for the case where the eigenpairs are approximated by the modified Steklov method. In Section 5 we provide the weak formulation for extracting the first derivatives when the solution is analytical inside the domain. It is shown also that our method is equivalent to one shown to be superconvergent in [9]. Section 6 contains the formulation for the extraction of the derivatives on curved boundaries.

2. Extraction procedures using the complementary weak form

Notation: Let Ω be a simply connected domain with boundaries $\partial\Omega = \cup_i \Gamma_i$ which are analytic simple arc curves called edges. These edges intersect at points called vertices. The Laplace problem $\nabla^2 u = 0$ is prescribed over Ω, with Dirichlet boundary conditions $u = \hat{u}$ on Γ^{D} and Neumann boundary conditions $\mathrm{d}u/\mathrm{d}\nu = \hat{t}$ on $\partial\Omega - \Gamma_i^{\mathrm{D}}$. Newton (also known as mixed) boundary conditions may be prescribed as well, but will not be considered here. Define the space $H_0^1(\Omega) = \{u \in H^1(\Omega) \mid u = 0 \text{ on } \Gamma_i^{\mathrm{D}}\}$.

In the displacement formulation, the exact solution of the problem is defined by the weak form (the primal weak form):

$$\begin{aligned} &\text{Find} && u \in H^1(\Omega), \qquad u = \hat{u} \quad \text{on } \Gamma^{\mathrm{D}} \\ &\text{Such that} && \mathcal{B}(u,v) = \mathcal{F}(v) \quad \forall v \in H_0^1(\Omega), \end{aligned} \tag{4}$$

where the bilinear form is

$$\mathcal{B}(u,v) = \int_\Omega \sum_{i=1}^{2} \frac{\partial u}{\partial x_i} \frac{\partial v}{\partial x_i} \, \mathrm{d}\Omega, \tag{5}$$

and the linear form is

$$\mathcal{F}(v) = \int_{\partial\Omega - \Gamma^{\mathrm{D}}} \hat{t} v \, \mathrm{d}s. \tag{6}$$

By $\|u\|_E = \sqrt{\mathcal{B}(u,u)}$ we denote the energy norm of u. Note that it is equivalent to the $H^1(\Omega)$ seminorm.

The exact solution u is analytic in Ω, except in the vicinity of the singular points (at the vertices), where the solution is given by the asymptotic expansion (1).

We use the p-version of the finite element method for approximating the solution of the weak form, i.e. we use a hierarchic sequence of finite element spaces $S_1(\Omega) \subset \cdots \subset S_i(\Omega) \subset H^1(\Omega)$. These finite element spaces consist of continuous piecewise polynomials of degree p on the elements of the mesh, such that the degree of the polynomial is increased as we go from S_i to S_{i+1}.

For the p-version it was shown in [17] that the error between the approximated finite element solution to the weak form (4), $u_{\mathrm{FE}}^{(i)} \in S_i$, and the exact solution u is given by

$$\|e\|_E \overset{\mathrm{def}}{=} \|u - u_{\mathrm{FE}}^{(i)}\|_E \leqslant C p_i^{-2\min(\alpha_n)} \approx \mathrm{O}(N^{-\min(\alpha_n)}), \tag{7}$$

where C is a constant, N is the total number of degrees of freedom and $p^2 \approx N$. With a proper (known) mesh refinement towards the singular point, the error in energy norm was shown to converge exponentially

$$\|e\|_E \leqslant C \exp(-\gamma N^{1/3}), \quad \gamma > 0. \tag{8}$$

It has been proven also that in the asymptotic range the estimates are sharp, meaning that the $\leqslant$ sign may be replaced by 'approximately equal' ($\approx$).

The polynomial approximation obtained by the finite element method does not account for the special form of the exact solution as being a span of harmonic functions in the interior of the domain, or eigenpairs near singular points, so that the approximation of the derivatives and the GFIFs may not be accurate at all. In the vicinity of point O, interior point (see Fig. 1), or point Q (laying on the smooth boundary), the exact solution u is analytical and can be expanded as an infinite sum:

$$u = \sum_{i=0}^{\infty} A_i z^i \quad \Rightarrow \quad u = \sum_{i=0}^{\infty} A_i r^i (\sin i\theta + \cos i\theta), \tag{9}$$

where r and θ are the polar coordinates of a system located in the points O or Q. The infinite series Eq. (9) converges absolutely. In the vicinity of the singular point P, the exact solution u can be expanded as shown in Eq. (1) (we exclude for the moment the special cases where the $\ln r$ terms appear)

$$u = \sum_{i=1}^{\infty} A_i r^{\alpha_i} \phi_i(\theta). \tag{10}$$

In the case of the Laplace equation, α_j and $f_j(\theta)$ can be computed exactly using analytic methods (where in the general case numerical approximations have to be sought). Both Eqs. (9) and (10) can be represented by Eq. (10), where $\phi_i(\theta)$ are analytic functions.

The following procedure is proposed: Assume that the first derivatives are sought in the points O or Q or the GFIFs corresponding to the point P. First we solve the problem over the entire domain Ω by means of the finite element method on the basis of the primal weak form (4), thus obtaining $u_{\mathrm{FE}}^{(i)}$. Second, a small subdomain around the point of interest is constructed. Define S_R as a circle of radius R

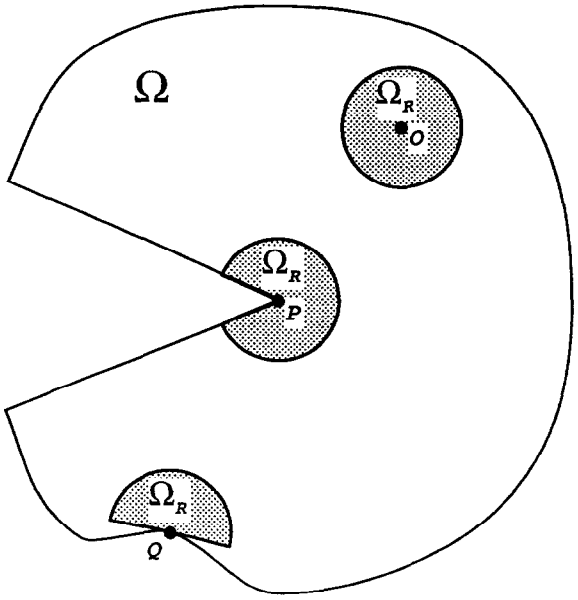

Fig. 1. Typical points of interest in a domain.

centered at points O, P or Q. The subdomain Ω_R is defined by $\Omega \cap S_R$. The flux vector is computed on S_R using the complementary weak form.

For the complementary weak form the trial and test spaces are chosen to be linear combinations of the derivatives of the eigenfunctions.

The approximated finite element solution, $u_{\mathrm{FE}}^{(i)}$, is applied on the boundary $\partial\Omega_R$ as the natural boundary conditions for the complementary problem. The finite element solution corresponding to the complementary weak form maximizes the complementary energy in Ω_R. Solving the finite element system of equation over Ω_R, one obtains an approximation for the series coefficients, thus, also the derivatives.

2.1. The complementary weak form

We define the vector space $E_c(\Omega_R)$ as follows:

$$E_c(\Omega_R) = \left\{ (q_x, q_y) \middle| \iint_{\Omega_R} |\boldsymbol{q}|^2 \, \mathrm{d}\Omega < \infty, \ \frac{\partial q_x}{\partial x} + \frac{\partial q_y}{\partial y} = 0 \right\}. \tag{11}$$

We define by Γ_q that part of the boundary of Ω_R where essential boundary condition for the complementary weak form ($q_n = \hat{q}$) is prescribed. The space of admissible fluxes is denoted by $\tilde{E}_c(\Omega_R)$ and is defined by

$$\tilde{E}_c(\Omega_R) = \left\{ (q_x, q_y), | (q_x, q_y) \in E_c(\Omega_R), \ q_n = \hat{q} \text{ on } \Gamma_q \right\}. \tag{12}$$

Note that if $(q_x, q_y) = (\partial u/\partial x, \partial u/\partial y)$, the condition $\partial q_x/\partial x + \partial q_y/\partial y = 0$ is nothing more than the Laplace equation itself. The complementary weak form is stated as follows:

$$\begin{array}{ll} \text{Find} & \boldsymbol{q} \in \tilde{E}_c(\Omega_R) \\ \text{Such that} & \mathcal{B}_c(\boldsymbol{q}, \boldsymbol{l}) = \mathcal{F}_c(\boldsymbol{l}) \quad \forall \boldsymbol{l} \in \tilde{E}_c(\Omega_R), \end{array} \tag{13}$$

where

$$\mathcal{B}_c(\boldsymbol{q}, \boldsymbol{l}) \equiv \iint_{\Omega_R} \boldsymbol{q} \cdot \boldsymbol{l} \ \mathrm{d}\Omega = \iint_{\Omega_R} (q_x l_x + q_y l_y) r \, \mathrm{d}r \, \mathrm{d}\theta, \tag{14}$$

and

$$\mathcal{F}_c(\boldsymbol{l}) \equiv \int_{\Gamma_{\hat{u}}} \hat{u}(\boldsymbol{l} \cdot \boldsymbol{\nu})\, \mathrm{d}s = \int_{\Gamma_{\hat{u}}} \hat{u}(l_x \cos\theta + l_y \sin\theta)\, \mathrm{d}s\,. \tag{15}$$

Detailed discussion on the complementary weak form and its relation to the primal weak form is given in [18], where it is shown that the exact energy can by bounded from below as well as from above by the approximated energy computed using the two weak forms. These bounds have been widely used for electromagnetic problems in which two finite element solutions were obtained over the same domain using both forms. The error in the energy was bounded by the finite element solutions (see [19] and references therein). These bounds, however, are global measures, which provide no information about the quality of the solution and its derivatives in specific points, and furthermore, each problem has to be solved twice which is not practical in general.

Our method is different from the method discussed above in that it is aimed at finding pointwise quantities *in the post-solution phase.*

2.2. Sources of discretization errors

We use only a *finite* number of *approximated eigenpairs* in the general case (except when the exact solution is analytical, where the eigenvalues are integers and the eigenfunctions are known exactly) instead of the infinite number of exact eigenpairs. As a result, the extraction method described herein has three sources of discretization errors:

(1) The fluxes are represented by a finite series of N terms. The exact representation is an infinite series.
(2) The eigenpairs are only an approximation of the exact values (except when the exact solution is analytical). In the general case, therefore, we do not satisfy the condition of static admissibility exactly.
(3) The boundary conditions are an approximation of the exact solution.

The first source of discretization error does not exist in the Laplace problem because the eigenpairs are orthogonal with respect to the bilinear form on Ω_R.

The second source of discretization error does not exist in case of the Laplace problem since the eigenpairs can be found analytically, thus do not have to be approximated. However, we shall demonstrate that an approximation of the eigenpairs (obtained by the modified Steklov method) is so accurate that the error is negligible for practical purposes.

REMARK 1. When the solution is smooth and analytical, we have shown in [12] that the direct method provides a good approximation to the derivatives, therefore indirect extraction may not be necessary.

REMARK 2. The proposed method does not distinguish between cases when the derivatives are sought *on* the boundaries or in the interior of the domain. Moreover, the proposed method is equally well suited for anisotropic domains [11]. Therefore, it may be implemented in any finite element code.

3. Extraction procedures in the vicinity of singular points

First we describe the computation of the coefficients of the asymptotic expansion in the vicinity of a reentrant corner using the exact eigenpairs. This eliminates the second source of discretization error. Consider, for example, a reentrant corner of $(2\pi - \omega)$ degrees, where (q_x, q_y) are computed in terms of the *exact eigenpairs*:

$$\boldsymbol{q} = \begin{Bmatrix} \dfrac{\partial u}{\partial x} \\ \dfrac{\partial u}{\partial y} \end{Bmatrix} = \begin{Bmatrix} \cos\theta \dfrac{\partial u}{\partial r} - \dfrac{\sin\theta}{r} \dfrac{\partial u}{\partial \theta} \\ \sin\theta \dfrac{\partial u}{\partial r} + \dfrac{\cos\theta}{r} \dfrac{\partial u}{\partial \theta} \end{Bmatrix}, \tag{16}$$

where u is given for 'free–free' boundary conditions (i.e. $q_n = 0$ on the reentrant straight boundaries) by

$$u = \sum_{n=0}^{\infty} A_n r^{\alpha_n} \cos(\alpha_n \theta), \qquad \alpha_n \overset{\text{def}}{=} n\pi/\omega, \tag{17}$$

therefore, Eq. (16) becomes

$$\boldsymbol{q} = \sum_{n=0}^{\infty} A_n \alpha_n r^{\alpha_n - 1} \begin{Bmatrix} \cos[(1-\alpha_n)\theta] \\ \sin[(1-\alpha_n)\theta] \end{Bmatrix}. \tag{18}$$

The elements of the compliance matrix $[B_c]$, which correspond to the bilinear form $\mathcal{B}_c(\boldsymbol{q}, \boldsymbol{l})$, are given by

$$(B_c)_{ij} = \int_0^R \int_0^{\omega} \alpha_i \alpha_j r^{\alpha_i + \alpha_j - 1} \cos[(\alpha_j - \alpha_i)\theta] \, \mathrm{d}r \, \mathrm{d}\theta. \tag{19}$$

Finally, after integrating, we have the following:

$$(B_c)_{ij} = \begin{cases} \dfrac{\alpha_i \alpha_j}{\alpha_i^2 - \alpha_j^2} R^{\alpha_i + \alpha_j} \sin[(\alpha_i - \alpha_j)\omega] & i \neq j \\ (\alpha_i/2) R^{2\alpha_i} \omega & i = j. \end{cases} \tag{20}$$

REMARK 3. The compliance matrix is diagonal, $(B_c)_{ij} = 0, \quad i \neq j$. For proof see [1, Section 12.1.2].

Consider now the expression for the linear form $\mathcal{F}_c$. This can be divided into two terms: One corresponding to the circular boundary called Γ_3, the other corresponding to the straight boundaries Γ_1 and Γ_2 which intersect in the singular point.

Assume that the solution on Γ_3 is given by $u|_{\Gamma_3} = \hat{u}(\theta)$:

$$\left(\mathcal{F}_c^{\Gamma_3}\right)(\boldsymbol{l}) = \int_{\Gamma_3} \hat{u}(\theta)(l_x \cos\theta + l_y \sin\theta) R \, \mathrm{d}\theta. \tag{21}$$

After substituting $\boldsymbol{l}$, which is in the form Eq. (18), Eq. (21) becomes

$$\left(\mathcal{F}_c^{\Gamma_3}\right)(\boldsymbol{l}) = \sum_{n=0}^{\infty} B_n \alpha_n R^{\alpha_n} \int_0^{\omega} \cos(\alpha_n \theta) \hat{u}(\theta) \, \mathrm{d}\theta. \tag{22}$$

The elements of the load vector $\{F_c^{\Gamma_3}\}$, which correspond to the linear form $\left(\mathcal{F}_c^{\Gamma_3}\right)(\boldsymbol{l})$ can be evaluated explicitly:

$$(F_c^{\Gamma_3})_i = \alpha_i R^{\alpha_i} \int_0^{\omega} \cos(\alpha_i \theta) \hat{u}(\theta) \, \mathrm{d}\theta. \tag{23}$$

For the case of 'free–free' boundary condition, $q_n = 0$ on Γ_1 and Γ_2. This condition, in the framework of the maximum complementary energy formulation, has to be treated by constraining the admissible trial function field. However, by using the exact eigenpairs in constructing the trial space, the constrains are automatically satisfied because the chosen $\boldsymbol{q}$ in Eq. (18) satisfies the condition $q_n = 0$ on Γ_1 and Γ_2.

In case of a 'fixed–free' boundary conditions (i.e. $u = 0$ on Γ_1 and $q_n = 0$ on Γ_2), u is given by

$$u = \sum_{n=1}^{\infty} A_n r^{\alpha_n} \sin(\alpha_n \theta), \qquad \alpha_n \overset{\text{def}}{=} (2n-1)\pi/2\omega. \tag{24}$$

The expression for $(B_c)_{ij}$ is identical to the one presented in Eq. (20), and the expression for $(F_c^{\Gamma_3})_i$ becomes

$$(F_c^{\Gamma_3})_i = \alpha_i R^{\alpha_i} \int_0^{\omega} \sin(\alpha_i \theta) \hat{u}(\theta)\, \mathrm{d}\theta. \tag{25}$$

THEOREM 1. The error in the load vector due to replacing u_{EX} with u_{FE} is bounded by the error in energy norm. $F_c(e) \leqslant C(R)\|e\|_E$.

PROOF. Consider a typical term in F_c corresponding to the kth eigenpair associated with $\mathcal{F}_c$:

$$\begin{aligned}(F_c(e))_k &\overset{\mathrm{def}}{=} \int_{\Gamma_3} (u - u_{\mathrm{FE}}) \frac{\partial (r^{\alpha_k} \phi_k(\theta))}{\partial \nu}\, \mathrm{d}s \\ &= \int_0^{\omega} e(\theta) \alpha_k R^{\alpha_k - 1} \phi_k(\theta) R\, \mathrm{d}\theta \\ &= C_1(R) \int_0^{\omega} e(\theta) \phi_k(\theta)\, \mathrm{d}\theta. \end{aligned} \tag{26}$$

$\phi_k(\theta)$ are analytic continuous functions on $\partial\Omega_R$, therefore they are bounded, $|\phi_k(\theta)| \leqslant M$, and Eq. (26) becomes

$$(F_c(e))_k \leqslant C_2(R) \int_0^{\omega} e(\theta)\, \mathrm{d}\theta \equiv C_2(R)\|e\|_{L_1(\Gamma_3)}.$$

Recall that $\|f\|_{L_r} \leqslant C_3\|f\|_{L_s}$, $s \geqslant r \geqslant 1$ we obtain

$$(F_c(e))_k \leqslant C_4(R)\|e\|_{L_2(\Gamma_3)} \leqslant C_5(R)\|e\|_{L_2(\partial\Omega_R)}.$$

We use the trace theorem now to obtain

$$(F_c(e))_k \leqslant C_6(R)\|e\|_{H^1(\Omega_R)} \leqslant C_7(R)\|e\|_{H^1(\Omega)}. \tag{27}$$

Using Friedrich's inequality, it is shown that the $H^1(\Omega_R)$ norm is equivalent to the $H^1(\Omega_R)$ seminorm for the Laplace problem, so we finally obtain

$$(F_c(e))_k \leqslant C(R)\|e\|_E. \quad \square \tag{28}$$

REMARK 4. When the compliance matrix is formulated using the exact eigenpairs, no discretization errors are associated with the compliance matrix of the complementary weak form. In view of Remark 3 (which holds true for singular points as well as points within the domain) we conclude that the convergence rate of the GFIFs and first derivatives at internal points is at least as fast as the energy norm.

The following numerical data indicate that errors in the computed GFIFs can converge much faster than the error in energy norm.

4. Numerical examples

The first numerical example is the same as the example in [9]. This particular example problem was chosen to demonstrate that the proposed method has the same superconvergent properties as the extraction method proposed by Babuška et al. [9]. The advantages of the proposed method are its generality with respect to its applicability to any singular point, and we do not have to construct a new auxiliary function to be tailored to the specific problem to be solved.

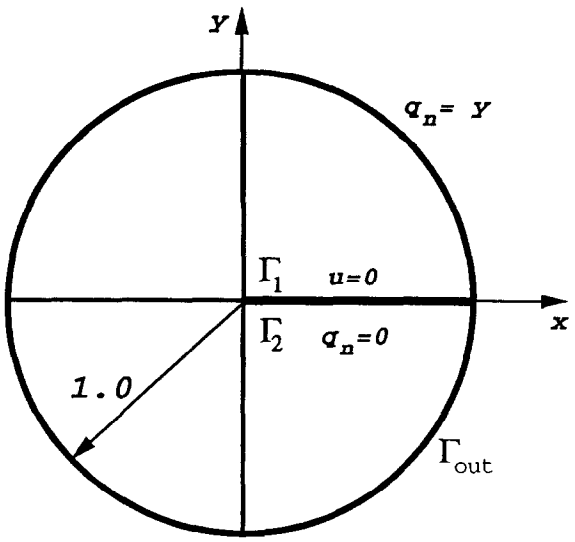

Fig. 2. The domain and notation for Babuška's model problem.

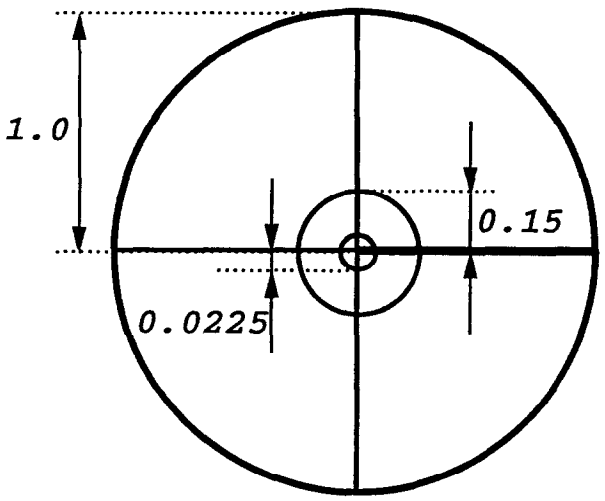

Fig. 3. The finite element mesh for Babuška's model problem.

Let Ω be the unit circle slit along the positive x axis. See Fig. 2. Consider the following model problem:

$$\begin{aligned} &\nabla^2 u = 0 && \text{in } \Omega \\ &u = 0 && \text{on } \Gamma_1 \\ &q_n = \frac{\partial u}{\partial \nu} = 0 && \text{on } \Gamma_2 \\ &q_n = \frac{\partial u}{\partial \nu} = y && \text{on } \Gamma_{\text{out}}. \end{aligned} \tag{29}$$

The first three exact GFIFs (correct to six significant figures) to this problem are $A_1 = -1.35812$, $A_2 = 0.970087$ and $A_3 = 0.452707$. The exact energy being $\int_\Omega |\nabla u|^2 \, dA = 4.52707$.

This problem has been solved using the p-version of the finite element method over the mesh shown in Fig. 3, having 2 refinements toward the singular point. The trunk space was used as the trial function space in all computations.

Table 1
Computed values of the first three GFIFs, $R = 0.9$ and $N = 10$

	p=1	p=2	p=3	p=4	p=5	p=6	p=7	p=8	p=∞
DOF	12	36	64	104	156	220	296	384	∞
$\|e\|_E$ (%)	34.5	16.7	12.8	11.3	10.3	9.5	8.9	8.4	0
$\hat{A}_1$	−1.106022	−1.26095	−1.28694	−1.30458	−1.31351	−1.31990	−1.32479	−1.32849	−1.35812
$e_{\hat{A}_1}$ (%)	−18.56	−7.15	−5.24	−3.94	−3.28	−2.81	−2.45	−2.18	0
$\hat{A}_2$	0.892975	0.970822	0.969563	0.970206	0.970089	0.970075	0.970091	0.970084	0.970087
$e_{\hat{A}_2}$ (%)	−7.9	0.075	−0.05	0.012	0.0002	−0.0012	0.0004	−0.0003	0
$\hat{A}_3$	0.378148	0.445853	0.452560	0.452493	0.452697	0.452704	0.452706	0.452707	0.452707
$e_{\hat{A}_3}$ (%)	−16.4	−1.5	−0.03	−0.047	−0.002	−0.0007	−0.0002	0	0

Table 2
Computed values of the first derivative, $R = 0.9$ and $N = 10$

	p=1	p=2	p=3	p=4	p=5	p=6	p=7	p=8	p=∞
DOF	12	36	64	104	156	220	296	384	∞
$\|e\|_E$ (%)	34.5	16.7	12.8	11.3	10.3	9.5	8.9	8.4	0
Direct:									
$\partial u/\partial x$ (0.01, −0)	19.18514	22.3081	18.4573	13.0017	11.8175	14.1345	15.5786	14.4513	12.8536
$e_{\partial u/\partial x}$ (%)	49.2	73.6	43.6	1.15	8.1	9.9	21.2	12.4	0
ASPP:									
$\partial u/\partial x$ (0.01, −0)	10.7082	12.0901	12.2897	12.4307	12.5009	12.5513	12.5901	12.619289	12.8536
$e_{\partial u/\partial x}$ (%)	−16.7	−5.94	−4.4	−3.3	−2.74	−2.35	−2.05	−1.8	0

Once the approximated GFIFs are obtained, the derivatives of the solution at any point in the vicinity of the singularity can be calculated using the asymptotic series. This method for calculating the derivatives will be called in the following ASPP (asymptotic series post-processing) method in contrast with the direct method.

Using the shown mesh, we extract the GFIFs on the path $R = 0.9$ having 10 terms in the series. In Table 1 we summarize the approximated first three GFIFs, the corresponding number of degrees of freedom, the relative error in energy norm, and in Table 2 the first derivative $\partial u/\partial x$ in the point $(x, y) = (0.01, -0.0)$ using both the direct and the AS post-processing methods.

The following conclusions may be drawn from the results shown in Tables 1 and 2 and other numerical experiments performed:

(1) Despite the presence of a strong ($r^{1/4}$-type) singularity, $\hat{A}_1$ appears to be converging at a rate which is at least twice as compared with the convergence rate of the error in energy norm. This rate of convergence is approximately the same as that reported in [9].
(2) The GFIFs $\hat{A}_2$ and $\hat{A}_3$ are much more accurate than $\hat{A}_1$ (the error is smaller than that reported in [9]), and the observed convergence rate is considerably faster when compared with the convergence of the error in energy norm.
(3) For path radii taken far enough from the singular point, $R > 0.5$ in this example problem, the accuracy of the GFIFs is almost independent of R.
(4) As expected, the number of terms considered in the series has no influence on the accuracy of the GFIFs.
(5) The pointwise first derivative ($\partial u/\partial x$) in the vicinity of the singular point computed by the ASPP method converge at least twice as fast as the error in the energy norm, while the direct method produces results of relatively low quality. See Fig. 4.
(6) The accuracy of the ASPP approximation for $\partial u/\partial x$ is affected by both the accuracy of the GFIFs used and the truncation error made by only considering the first N terms of the asymptotic expansion. However, the proposed method provides any number of N terms as desired, thus, N can be taken sufficiently large so that the truncation error is negligible.

We present in Fig. 5 the convergence of the GFIFs as compared with the relative error in energy norm and the relative error in strain energy. Note that the rate of convergence in the first GFIF is

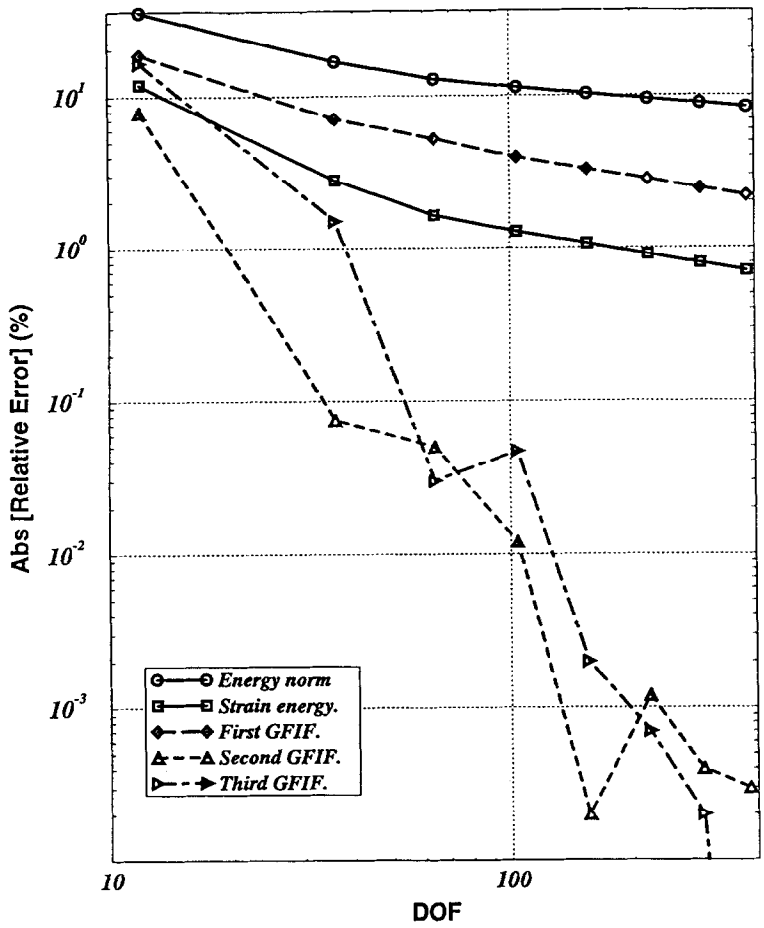

Fig. 4. Convergence of the relative error in energy norm and the first derivative ($x = 0.01, y = -0$) for Babuška's problem.

faster than the rate of convergence of the energy norm, and at $p > 4$ is virtually the same as the rate of convergence of the strain energy. The second and third GFIFs converge much faster. This is because the corresponding eigenfunctions are much smoother.

It is seen that the first GFIF and the first pointwise derivatives converge monotonically, which should not be expected in general.

4.1. The approximated asymptotic expansion

In general scalar elliptic problems the exact eigenpairs are not known, and the Steklov method or the modified Steklov method [20] has to be applied over Ω_R, so that an approximation of the eigenpairs is obtained. The finite element solution for each p level, u_{FE}, can then be represented by the linear combination with unknown coefficients $\hat{A}_j$:

$$u_{\mathrm{FE}} = \sum_{j=1}^{\infty} \hat{A}_j r^{\hat{\alpha}_j} \hat{\phi}_j(\theta)\,. \tag{30}$$

The functions $\hat{\phi}_j(\theta)$ are given in terms of the shape function on the edge as

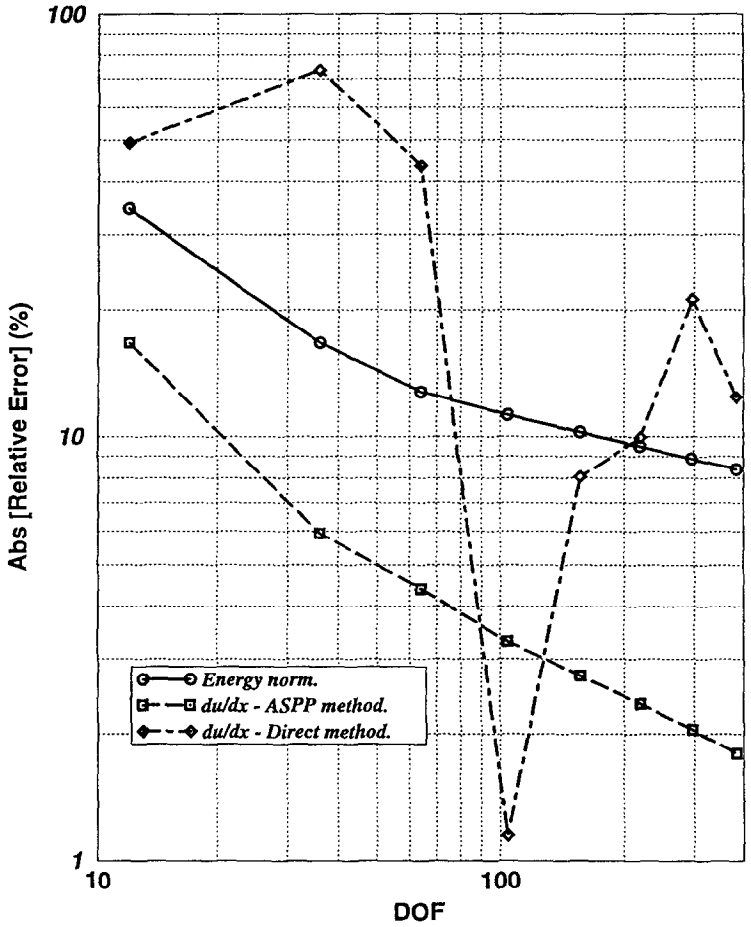

Fig. 5. Convergence of the relative error in energy norm, strain energy and the GFIFs for Babuška's problem.

$$\hat{\phi}_j(\theta(\xi)) = \sum_{i=1}^{p+1} c_{ij} N_i(\xi)\,,$$

where $N_i(\xi)$ are integrals of Legendre polynomials for $i \geqslant 3$.

The Steklov method solved by the finite element method ensures the convergence of the eigenpairs with respect to increasing degrees of freedom (DOF):

$$\lim_{\mathrm{DOF}\to\infty} \left(\hat{\alpha}_j, \hat{\phi}_j(\theta)\right) = \left(\alpha_j, \phi_j(\theta)\right), \tag{31}$$

so that the flux vector computed from the approximated eigenpairs, in the limit, belongs to the space $\tilde{E}_c(\Omega_R)$. It is not difficult to show that the resulting flux vectors are square integrable.

In the following, we formulate the complementary weak form for the case where the eigenpairs are only an approximation of the exact values. These approximations are obtained using the modified Steklov method reported in [6], where we show that an excellent approximation can be achieved with a small effort. We examine this case since in general elliptic problems, including the elasticity problems, the eigenpairs cannot by computed analytically for general singular points when the materials are anisotropic.

We now formulate the variational formulation explicitly. Based on Eq. (30), we obtain

$$\begin{Bmatrix} q_x \\ q_y \end{Bmatrix} = \sum_{j=1}^{\infty} \hat{A}_j r^{\hat{\alpha}_j - 1} \begin{Bmatrix} \sum_{i=1}^{p+1} c_{ij} \left(\hat{\alpha}_j N_i(\theta) \cos\theta - \dfrac{\mathrm{d}N_i(\theta)}{\mathrm{d}\theta} \sin\theta \right) \\ \sum_{i=1}^{p+1} c_{ij} \left(\hat{\alpha}_j N_i(\theta) \sin\theta + \dfrac{\mathrm{d}N_i(\theta)}{\mathrm{d}\theta} \cos\theta \right) \end{Bmatrix}. \tag{32}$$

The expression for the complementary bilinear form is based on Eq. (14), and after substituting Eq. (32) we obtain

$$\begin{aligned} \mathcal{B}_c(\boldsymbol{q}, \boldsymbol{q}) &= \int_{\theta_1}^{\omega} \int_0^R (q_x^2 + q_y^2) r \, \mathrm{d}r \, \mathrm{d}\theta \\ &= \sum_{j,\ell=1}^{N} \hat{A}_j \hat{A}_\ell \frac{R^{\hat{\alpha}_j + \hat{\alpha}_\ell}}{(\hat{\alpha}_j + \hat{\alpha}_\ell)} \sum_{i,k=1}^{p+1} \int_{\theta_1}^{\omega} \left[\hat{\alpha}_j \hat{\alpha}_\ell N_i N_k + N_i' N_k' \right] c_{ij} c_{k\ell} \, \mathrm{d}\theta. \end{aligned} \tag{33}$$

Assume that the finite element mesh used for computing the eigenpairs has nG elements in the circumferential direction and a polynomial degree p. Using a Gauss quadrature of N_G points, the explicit expression for each term in the compliance matrix is given by

$$\begin{aligned} (B_c)_{ij} = \frac{R^{\hat{\alpha}_i + \hat{\alpha}_j}}{(\hat{\alpha}_i + \hat{\alpha}_j)} \sum_{n=1}^{nG} \hat{\alpha}_i \hat{\alpha}_j \sum_{k,\ell=1}^{p+1} c_{ik}^{(n)} c_{j\ell}^{(n)} \Bigg[\left(\frac{\omega^{(n)} - \theta_1^{(n)}}{2} \sum_{m=1}^{N_G} W_m N_k(\xi_m) N_\ell(\xi_m) \right) \\ + \left(\frac{2}{\omega^{(n)} - \theta_1^{(n)}} \sum_{m=1}^{N_G} W_m N_k'(\xi_m) N_\ell'(\xi_m) \right) \Bigg], \end{aligned} \tag{34}$$

where W_m and ξ_m are the weights and abscissas of the Gauss quadrature and nG is the number of partitions used for computing the approximated eigenpairs (see [11] for details).

REMARK 5. $(B_c)_{ij} = c_i \delta_{ij}$, therefore only the diagonal terms are to be computed. The values $(B_c)_{ij}$, $i \neq j$ are computed also, to assess the accuracy of the approximated eigenpairs.

We proceed now to the evaluation of the linear form corresponding to the principle of maximum complementary energy. Consider first the term corresponding to Γ_3.

Substituting Eq. (32) in Eq. (15) the linear form corresponding to Γ_3 becomes

$$\mathcal{F}_c^{\Gamma_3}(\boldsymbol{q}) = \int_{\theta_1}^{\omega} \hat{u}(\theta) \left[\sum_{j=1}^{N} \hat{A}_j \hat{\alpha}_j R^{\hat{\alpha}_j} \sum_{i=1}^{p+1} c_{ij} N_i(\theta) \right] \mathrm{d}\theta. \tag{35}$$

The explicit expression for each term in the load vector is given by

$$(F_c)_i = \hat{\alpha}_i R^{\hat{\alpha}_i} \sum_{n=1}^{nG} \sum_{k=1}^{p+1} c_{ik}^{(n)} \frac{\omega^{(n)} - \theta_1^{(n)}}{2} \sum_{m=1}^{N_G} W_m N_k(\xi_m) \hat{u}(\theta(\xi_m)). \tag{36}$$

The boundary conditions on Γ_1 and Γ_2 are fulfilled automatically because the approximated eigenpairs satisfy them.

Note that the finite element discretization over the domain Ω may be different from the one used for the modified Steklov problem.

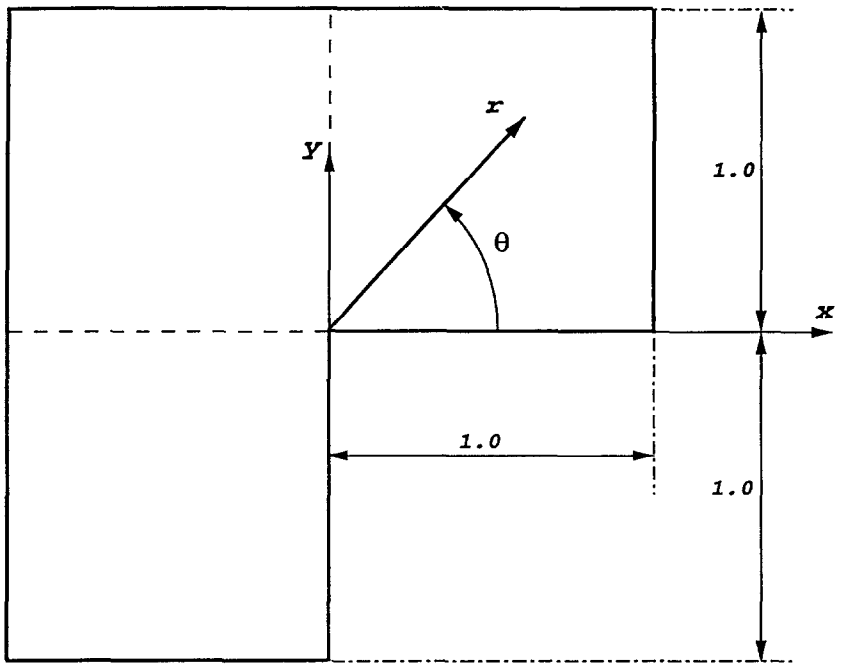

Fig. 6. The L-shaped example problem and the finite element mesh.

4.2. Numerical example

The example discussed in this subsection is constructed so that the exact solution is known. It demonstrates: (a) the influence of the approximated eigenpairs, obtained using the modified Steklov method, on the accuracy of the extracted GFIFs; (b) the performance and efficiency of the proposed extraction method.

We consider a 90° V-notch in an infinite domain. We 'remove' the L-shaped domain shown in Fig. 6, and impose on its boundaries the Neumann boundary conditions corresponding to the exact analytic solution, which is known. The exact asymptotic solution for this free-free V-notch is given by Eq. (17) and the derivatives in x and y directions (q_x, q_y) to be imposed on the boundaries of the L-shaped domain are given by Eq. (18).

First, an approximation to the eigenpairs has to be obtained. The modified Steklov method is used over a mesh containing two elements shown in Fig. 7. As the p-level of the shape functions is increased over the mesh in Fig. 7, a better approximation of the eigenpairs is obtained. We will use the eigenpairs obtained when assigning p-levels 4, 5, 6, 7 and 8 for the computation of the approximated GFIFs.

Once the approximated eigenpairs are available, a finite element solution is sought for the L-shaped domain. We construct a mesh containing the minimum possible number of elements over the L-shaped domain without any refinements in the vicinity of the singular point, as shown in Fig. 6. The boundary conditions in Eq. (18) were imposed on the L-shaped boundaries, with the GFIFs chosen to be: $A_1 = 1$, $A_2 = 1/2, A_3 = 1/3, A_4 = 1/4, A_5 = 1/5$ and $A_i = 0, (i = 6, 7, \ldots)$. The GFIFs were then extracted using our proposed method, taking R to be 0.9. The results of these computations are displayed in Table 3. The following conclusions may be drawn from the results shown in Table 3:

(1) The errors in the approximated ith eigenpair do not influence the accuracy of the jth GFIF. This is because the eigenfunctions are orthogonal.
(2) The error in the GFIFs is always bounded by the error in energy norm when the error in the

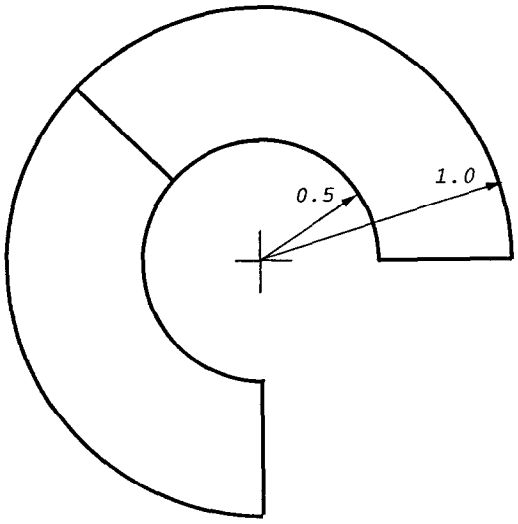

Fig. 7. Mesh for the computation of the approximated eigenpairs.

eigenpairs is less than 0.1%. Moreover, in this case the error in the GFIFs is virtually the same as if the exact eigenvalues had been used to extract the GFIFs.

(3) Using the coarsest mesh possible for the extraction of both the eigenpairs and the GFIFs, excellent results have been obtained. The relative error in the first 5 eigenpairs is less than 0.007%, and the relative error in the first 5 GFIFs is less than 0.7% when the relative error in energy norm is 2.6%.

The eigenpairs together with the computed GFIFs can be used for computing the solution and the first derivatives in the neighborhood of the singular point. The procedure is straightforward and is based on Eq. (32) for the derivatives and on Eq. (30) for the solution. This extraction method was denoted in the previous section as the 'ASPP' method. The eigenpairs corresponding to p-level = 8 were used in our computation, and we examine the values at the point $(x,y) = (0.1,0)$. The exact values are $u_{EX} = 0.242616185$ and $(\partial u/\partial x)_{\mathrm{EX}} = 1.8298530$. The error in the computed values is compared with the error in the values computed directly in Table 4. The values in Table 4 are shown graphically in Figs. 8 and 9. The derivatives obtained by the ASPP method using the approximated eigenpairs, have the same convergence properties as in the previous section, namely, convergence is much faster than the error in energy norm and the extracted values using the direct method.

5. Extraction procedures when the solution is analytic

In this section we provide the explicit formulation for the complementary weak form to be used for extracting the first derivatives at interior points, and show that our method yields the same formulation as presented in [13]. Therefore, our method is superconvergent.

The solution is analytical in the neighborhood of the point O (see Fig. 1). In this case, the solution for $\nabla^2 u = 0$, can be expanded in an infinite series of the form:

$$u = \sum_{n=0}^{\infty} A_n r^n [\sin(n\theta) + \cos(n\theta)], \tag{37}$$

where r, θ are polar coordinates of a system located in point O. In this case if we take $(q_x, q_y) = (\partial u/\partial x, \partial u/\partial y)$, then $(q_x, q_y) \in \tilde{E}_c(\Omega_R)$.

Table 3
Relative error (%) in computed GFIFs for the L-shaped domain

p-level for eigenvalue computation	GFIF #	Error in eigenvalue	$\|e\|_E$	p=4 6.02	p=5 4.65	p=6 3.74	p=7 3.10	p=8 2.62	Extrapolated
	$\hat{A}_1$	0.0002		−1.63	−0.75	−0.38	−0.45	−0.31	−0.5
	$\hat{A}_2$	0.03		0.54	0.36	0.36	0.42	0.41	0.4
p=4	$\hat{A}_3$	0.39		6.79	6.84	6.87	6.87	6.84	6.87
	$\hat{A}_4$	0.73		7.12	7.68	7.64	7.52	7.56	7.56
	$\hat{A}_5$	17		28.5	25.55	26.15	34.4	26.8	26.85
	$\hat{A}_1$	$3 \cdot 10^{-6}$		−1.62	−0.73	−0.36	−0.43	−0.30	−0.48
	$\hat{A}_2$	$3 \cdot 10^{-5}$		0.12	−0.064	−0.064	0.001	−0.0096	−0.016
p=5	$\hat{A}_3$	0.035		0.54	0.63	0.61	0.61	0.61	0.62
	$\hat{A}_4$	0.71		7.2	7.76	7.72	7.6	7.64	7.6
	$\hat{A}_5$	2.4		29.5	26.65	27.5	28.7	28.1	28.35
	$\hat{A}_1$	$4.5 \cdot 10^{-8}$		−1.62	−0.73	−0.37	−0.43	−0.29	−0.48
	$\hat{A}_2$	$2.25 \cdot 10^{-5}$		0.122	−0.058	−0.058	0.0066	−0.0044	−0.01
p=6	$\hat{A}_3$	0.0018		−0.216	−0.135	−0.138	−0.160	−0.17	−0.147
	$\hat{A}_4$	0.0084		−0.52	0.009	−0.044	−0.136	−0.112	−0.116
	$\hat{A}_5$	0.49		6.2	3.6	4.19	5.05	4.69	4.77
	$\hat{A}_1$	$< 10^{-9}$		−1.62	−0.73	−0.37	−0.43	−0.29	−0.48
	$\hat{A}_2$	$3 \cdot 10^{-8}$		0.13	−0.05	−0.05	−0.016	0.005	−0.001
p=7	$\hat{A}_3$	$7.8 \cdot 10^{-5}$		−0.08	−0.01	−0.0048	−0.027	−0.037	−0.037
	$\hat{A}_4$	0.0069		−0.71	−0.184	−0.235	−0.326	−0.302	−0.304
	$\hat{A}_5$	0.063		1.235	−1.235	−0.639	−0.212	−0.173	−0.0825
	$\hat{A}_1$	$< 10^{-9}$		−1.62	−0.73	−0.37	−0.43	−0.30	−0.48
	$\hat{A}_2$	$< 10^{-9}$		0.13	−0.05	−0.05	0.016	0.0046	−0.0015
p=8	$\hat{A}_3$	$2.3 \cdot 10^{-6}$		−0.058	0.021	0.027	0.004	−0.0055	0.009
	$\hat{A}_4$	$3.7 \cdot 10^{-5}$		−0.427	0.099	0.047	−0.044	−0.021	−0.022
	$\hat{A}_5$	0.0064		2.07	−0.436	0.155	1.0	0.63	0.715
	$\hat{A}_1$	0		−1.63	−0.73	−0.36	−0.43	−0.30	−0.48
	$\hat{A}_2$	0		−1.34	−0.05	−0.05	−0.014	−0.004	−0.016
p=∞	$\hat{A}_3$	0		0	0	0	0	0	0
	$\hat{A}_4$	0		−0.41	0.108	0.056	−0.03	−0.0096	−0.011
	$\hat{A}_5$	0		1.5	−0.92	−0.33	0.49	0.105	0.207

Table 4
Relative error (%) in u and $\partial u/\partial x$ at the point (0.1,0) for the L-shaped domain

	$\|e\|_E$	p=4 6.02	p=5 4.65	p=6 3.74	p=7 3.10	p=8 2.62
Direct:	u	−22.3	−16.8	−11.8	−7.9	−4.95
	$\partial u/\partial x$	1.63	6.66	9.67	10.72	10.25
ASPP:	u	−1.42	−0.66	−0.33	−0.38	−0.26
	$\partial u/\partial x$	−1.25	−0.58	−0.29	−0.18	−0.23

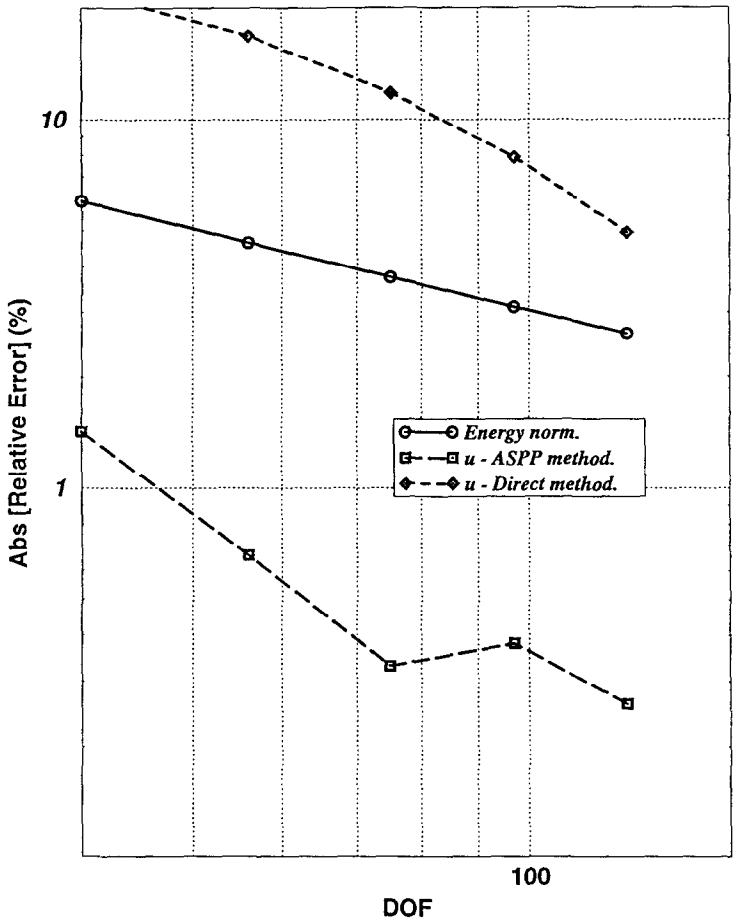

Fig. 8. Convergence of the relative error in energy norm and u at (0.1,0) for the L-shaped problem.

If we follow the same steps as presented through Eqs. (16)–(23), we obtain the compliance matrix entries to be

$$(B_c)_{ij} = \begin{cases} 0 & i \neq j \\ 2i\pi R^i & i = j, \end{cases} \tag{38}$$

and the entries of the load vector are explicitly evaluated:

$$(F_c)_i = iR^i \int_0^{2\pi} [\sin(i\theta) + \cos(i\theta)]\, \hat{u}(\theta)\, \mathrm{d}\theta. \tag{39}$$

The compliance matrix is diagonal, so the coefficients of the series can be evaluated explicitly:

$$A_i = \frac{1}{2\pi R^i} \int_0^{2\pi} [\sin(i\theta) + \cos(i\theta)]\, \hat{u}(\theta)\, \mathrm{d}\theta. \tag{40}$$

5.1. Superconvergent property

In the following we prove that the extraction of the coefficient A_1 by the complementary energy method (when the solution is analytical) is identical to the *superconvergent* extraction method, using auxiliary functions, proposed by Babuška et al. in [13]. Therefore, the complementary energy method has same convergence properties, i.e. is *superconvergent.*

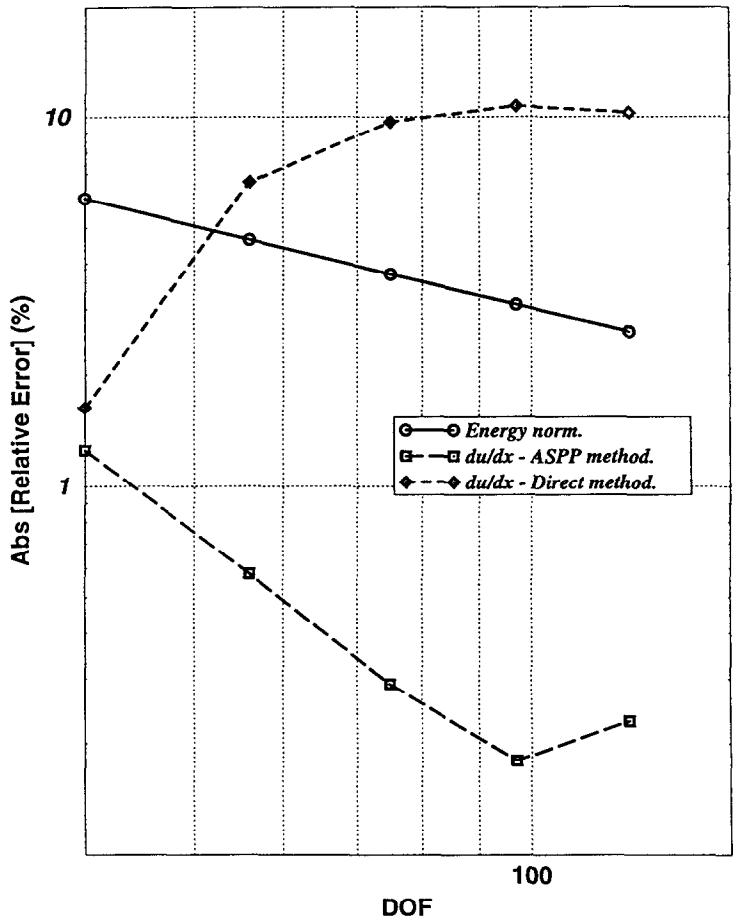

Fig. 9. Convergence of the relative error in energy norm and $\partial u/\partial x$ at (0.1, 0) for the L-shaped problem.

Given the domain Ω, let us choose the circular subdomain Ω_i of radius R around the point of interest P_0 obtaining the following problem:

$$\nabla^2 u = 0 \quad \text{in } \Omega_i\,, \tag{41}$$

and

$$u = \hat{u}(\theta) \quad \text{on } \partial\Omega_i. \tag{42}$$

Define now a circular subdomain S_ϵ of radius ϵ around the point of interest P_0, as shown in Fig. 10. Multiply Eq. (41) by a function ϕ, and integrate over $\Omega_i - S_\epsilon$

$$\int_{\Omega_i - S_\epsilon} \phi \nabla^2 u \, \mathrm{d}A = 0\,, \tag{43}$$

or

$$\int_{\Omega_i} \phi \nabla^2 u \, \mathrm{d}A - \int_{S_\epsilon} \phi \nabla^2 u \, \mathrm{d}A = 0\,. \tag{44}$$

Using Green's theorem

$$\int_A f \nabla^2 g \, \mathrm{d}A = \int_A g \nabla^2 f \, \mathrm{d}A + \int_{\partial A} \left(f \frac{\partial g}{\partial n} - g \frac{\partial f}{\partial n} \right) \mathrm{d}s\,,$$

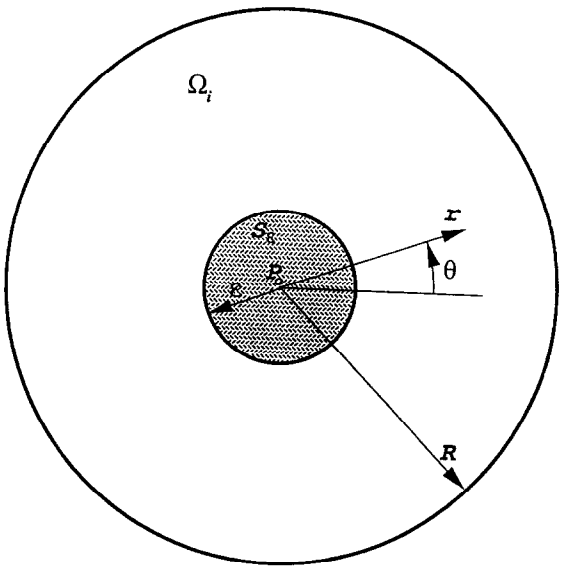

Fig. 10. The domain and notation for the extraction method based on an auxiliary function.

for both terms in Eq. (44), we obtain

$$\int_{\Omega_i} u\nabla^2\phi \, dA + \int_{\partial\Omega_i} \left(\phi \frac{\partial u}{\partial n} - u\frac{\partial \phi}{\partial n}\right) ds - \int_{S_\epsilon} u\nabla^2\phi \, dA - \int_{\partial S_\epsilon} \left(\phi \frac{\partial u}{\partial n} - u\frac{\partial \phi}{\partial n}\right) ds = 0. \tag{45}$$

We choose an auxiliary function (also called the extraction function) to be

$$\phi = \frac{1}{2\pi}\frac{g(\theta)}{r}, \tag{46}$$

so that

$$\nabla^2\phi = \frac{1}{2\pi}\left\{\frac{1}{r}\frac{\partial}{\partial r}\left(r\frac{-g(\theta)}{r^2}\right) + \frac{1}{r^2}\frac{g''(\theta)}{r}\right\} = \frac{1}{2\pi r^3}\left[g(\theta) + g''(\theta)\right]. \tag{47}$$

If $g(\theta) = \cos\theta$ or $\sin\theta$ then $\nabla^2\phi \equiv 0$, and the first and third expression in Eq. (45) vanish. Evaluating now the integrand of the second and fourth terms of Eq. (45) we obtain

$$\phi\frac{\partial u}{\partial r} - u\frac{\partial \phi}{\partial r} = \frac{1}{2\pi}\sum_{n=0}^{\infty} A_n(n+1)r^{n-2}g(\theta)\left[\sin(n\theta) + \cos(n\theta)\right]. \tag{48}$$

Substituting Eq. (48) in Eq. (45) and taking the limit as $\epsilon \to 0$ we obtain

$$\begin{aligned}\lim_{\epsilon\to 0}\int_{\partial S_\epsilon}\left(\phi\frac{\partial u}{\partial r} - u\frac{\partial\phi}{\partial r}\right) ds = \lim_{\epsilon\to 0}\frac{1}{2\pi}\Bigg\{&\int_0^{2\pi} A_0\epsilon^{-1}g(\theta)\,d\theta + \int_0^{2\pi} 2A_1 g(\theta)\left[\sin\theta + \cos\theta\right] d\theta \\ &+ \sum_{n=2}^{\infty}\epsilon^n\int_0^{2\pi} A_n g(\theta)\left[\sin n\theta + \cos n\theta\right)] \, d\theta\Bigg\}.\end{aligned} \tag{49}$$

The first term in Eq. (49) vanishes because $\int_0^{2\pi} g(\theta)\,d\theta = 0$ for $g(\theta) = \sin\theta$ or $g(\theta) = \cos\theta$. The last term in Eq. (49) vanishes because $\epsilon^n = 0$ for $\epsilon \to 0$, $n \geqslant 2$, so that Eq. (49) becomes

$$\frac{1}{\pi}\int_0^{2\pi} A_1 g(\theta)\left[\sin\theta + \cos\theta\right] d\theta = A_1, \qquad \text{for } g(\theta) = \sin\theta \text{ or } g(\theta) = \cos\theta. \tag{50}$$

Examine now the first part of the second term of Eq. (45):

$$\int_{\partial\Omega} \phi \frac{\partial u}{\partial n}\,\mathrm{d}s = \frac{1}{2\pi}\int_0^{2\pi} \sum_{n=0}^{\infty} A_n n R^{n-1} g(\theta)\,[\sin(n\theta) + \cos(n\theta)]\,\mathrm{d}\theta, \tag{51}$$

which after some algebraic manipulations becomes

$$\int_{\partial\Omega} \phi \frac{\partial u}{\partial n}\,\mathrm{d}s = \frac{A_1}{2} \tag{52}$$

for either $g(\theta) = \sin\theta$ or $g(\theta) = \cos\theta$.

Substituting Eqs. (50) and (52) in Eq. (45) we finally get

$$\frac{A_1}{2} - \int_{\partial\Omega} u \frac{\partial \phi}{\partial n}\,\mathrm{d}s - A_1 = 0,$$

or

$$A_1 = -2\int_{\partial\Omega} u \frac{\partial \phi}{\partial n}\,\mathrm{d}s = \frac{1}{\pi R}\int_0^{2\pi} g(\theta)\hat{u}(\theta)\,\mathrm{d}\theta. \tag{53}$$

Letting $g(\theta) = \cos\theta + \sin\theta$ we finally obtain:

$$A_1 = \frac{1}{2\pi R}\int_0^{2\pi} [\sin\theta + \cos\theta]\hat{u}(\theta)\,\mathrm{d}\theta, \tag{54}$$

which is identical to the expression obtained for A_1, using our method.

REMARK 6. The same procedure can be used to show that our expression for the GFIFs (at point O) is identical to the one presented by the contour integral method in [1]. In this case the extraction function for the ith GFIF is taken to be the ith eigenfunction with the $-\alpha_i$ eigenvalue.

6. First derivatives on curved edges

The method presented in previous section can by used for extracting the first derivatives at points on the boundaries. Let us attach a coordinate system in the point of interest Q, which lies on the boundary of the domain Ω, such that the x axis coincides with the normal vector and the y axis coincides with the tangential vector, see Fig. 11. The domain Ω_R is defined as $S_R \cap \Omega \cap \{x \geqslant 0\}$.

Assume that no abrupt changes occur in the boundary conditions in the vicinity of the point Q. Therefore, the solution in the neighborhood is analytical and can be expanded as in Eq. (37). Take again $\boldsymbol{q} \overset{\text{def}}{=} (q_x, q_y)^{\mathrm{T}} = (\partial u/\partial x,\ \partial u/\partial y)$, we may represent the space of kinematically admissible functions as follows:

$$\begin{aligned}\boldsymbol{q} = {} & A_1\begin{Bmatrix}1\\0\end{Bmatrix} + A_2\begin{Bmatrix}0\\1\end{Bmatrix} + A_3\begin{Bmatrix}r\cos(\theta)\\0\end{Bmatrix} + A_4\begin{Bmatrix}0\\r\sin(\theta)\end{Bmatrix} \\ & + A_5\begin{Bmatrix}r\sin(\theta)\\-r\cos(\theta)\end{Bmatrix} + A_6\begin{Bmatrix}r^2\cos 2\theta\\-r^2\sin 2\theta\end{Bmatrix} + A_7\begin{Bmatrix}r^2\sin 2\theta\\r^2\cos 2\theta\end{Bmatrix}\cdots.\end{aligned} \tag{55}$$

The bilinear form $\mathcal{B}_c(\boldsymbol{q}, \boldsymbol{q})$ can be evaluated by

$$\begin{aligned}\int_{-\pi/2}^{\pi/2}\int_{r=0}^{R} \Big[& \left(A_1 + A_3 r\cos\theta + A_5 r\sin\theta + A_6 r^2\cos 2\theta + A_7 r^2\sin 2\theta + \cdots\right)^2 \\ & + \left(A_2 + A_4 r\sin\theta - A_5 r\cos\theta - A_6 r^2\sin 2\theta + A_7 r^2\cos 2\theta + \cdots\right)^2\Big]\, r\,\mathrm{d}r\,\mathrm{d}\theta.\end{aligned} \tag{56}$$

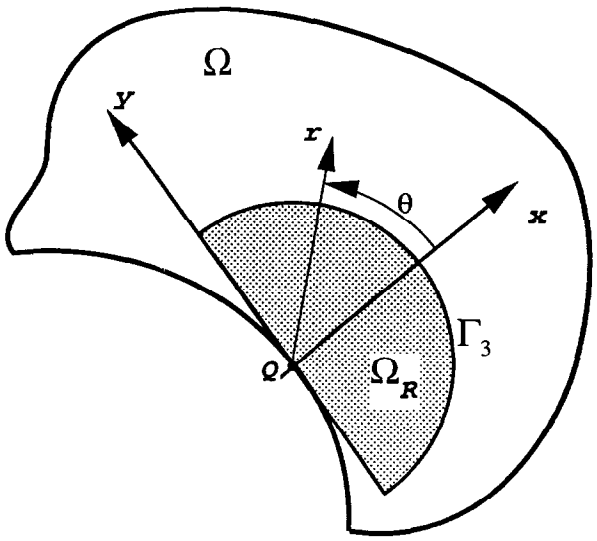

Fig. 11. Notations for derivatives extraction on curved boundaries.

The compliance matrix corresponding to the bilinear form consists of nothing more than integrals over trigonometric monomial functions, and is no longer diagonal because the trigonometric monomial functions are not orthogonal with respect to this specific bilinear form.

Assume that the solution on $\partial\Omega_R$ is given by $\hat{u}(\theta)$, then the expression for the linear form $\mathcal{F}_c$ is given by

$$(\mathcal{F}_c)(\boldsymbol{q}) = \int_{-\pi/2}^{\pi/2} \hat{u}(R,\theta)\left[(q_x\cos\theta + q_y\sin\theta)\right]_R R\,\mathrm{d}\theta - \int_{r=-R}^{0} \hat{u}(r,-\pi/2)[q_x]_{(-\pi/2)}\,\mathrm{d}r - \int_{r=0}^{R} \hat{u}(r,\pi/2)[q_x]_{(\pi/2)}\,\mathrm{d}r. \tag{57}$$

As previously explained, $\hat{u}(\theta)$ is replaced by the finite element solution u_{FE}, and the linear form $\mathcal{F}_c$ can be computed by a Gauss quadrature. The overall system is then solved to obtain the coefficients A_i, thus the derivatives at the point Q.

REMARK 7. The first derivatives in point Q are easily obtained because they are represented by the constants A_1 and A_2 alone, and the rest of the series (55) vanishes at $r = 0$.

REMARK 8. The accuracy of the coefficients A_i, $i \geqslant 3$, depends on the number of terms considered in the series Eq. (55). This is because the compliance matrix is fully populated. However, numerical experiments reported in [8] show that for relatively small number of coefficients good accuracy can be achieved.

7. Summary and conclusions

A superconvergent method for the computation of the GFIFs and first derivatives from finite element solutions was presented on the basis of the Laplace problem in two dimensions. Mathematical analysis and numerical examples demonstrated the efficiency and accuracy of the results. It was demonstrated that the computed values converge to the exact ones as fast as the energy norm, or faster.

The major advantages of the proposed method over the existing ones are as follows:

(1) The error in the pointwise data of interest exhibits superconvergence.

(2) The method is general, in the sense that it is applicable to any point of the domain using the same algorithm.

(3) The method is applicable to anisotropic materials, and any type of singularities. Numerical examples demonstrating the superconvergent behavior for anisotropic materials can be found in [11].
(4) Mathematical analysis and numerical experiments for the Steklov method applied to vertex singularities for Laplace's problem in three dimensions is provided in [5]. Therefore, the extension of the present method, for extracting GFIFs, to three dimensions is straightforward.
(5) The method can be used in conjunction with any finite element analysis program.

One obvious application of this method is to compute the error indicators in adaptive processes. The error indicators can be computed element by element, or for any group of elements. The indicators based on the difference between the complementary energy and the strain energy are expected to show relative error contributions for elements.

Acknowledgement

The support of this work by the Air Force Office of Scientific Research under grant No. F49620-93-1-0173 and grant No. 92-J-0043 is gratefully acknowledged. The writers thank Professor Ivo Babuška of the University of Texas at Austin for helpful discussions and advice.

References

[1] B.A. Szabó and I. Babuška, Finite Element Analysis (Wiley, New York, 1991).
[2] P. Grisvard, Elliptic Problems in Nonsmooth Domains (Pitman Publishing, England, 1985).
[3] P. Papadakis, Computational aspects of the determination of the stress intensity factors for two-dimensional elasticity, Ph.D. Dissertation, University of Maryland, 1988.
[4] D. Leguillon and E. Sanchez-Palencia, Computation of Singular Solutions in Elliptic Problems and Elasticity (Wiley, New York, 1987).
[5] V.A. Kondratiev, Boundary value problems for elliptic equations in domains with conical or angular points, Transact. Moscow Math. Soc. 16 (1967) 227–313.
[6] Z. Yosibash and B.A. Szabó, Numerical analysis of singular points, in: P.K. Basu and A. Nagar, eds., Recent Developments in Computational Mechanics, Volume 39 (ASME Press, 1993) 29–44.
[7] B.A. Szabó and I. Babuška, Computation of the amplitude of stress singular terms for cracks and reentrant corners, in: T.A. Cruse, ed., Fracture Mechanics: 19th Symposium (ASTM STP 969, Philadelphia, PA, 1988) 101–124.
[8] Z. Yosibash and B. Schiff, A superelement for two-dimensional singular boundary value problem in linear elasticity, Int. J. Fract. 62 (1993) 325–340.
[9] I. Babuška and A. Miller, The post processing approach in the finite element method, Part 2: The calculation of stress intensity factors, Int. J. Numer. Methods Engrg. 20 (1984) 1111–1129.
[10] L. Banks-Sills and D. Sherman, Comparison of methods for calculating stress intensity factors with quarter-point elements, Int. J. Fract. 32 (1986) 127–140.
[11] Z. Yosibash, Numerical analysis of singularities and first derivatives for elliptic boundary value problems in two dimensions, D.Sc. Dissertation, Sever Institute of Technology, Washington University, St. Louis, MO, USA, 1994.
[12] Z. Yosibash and B.A. Szabó, Convergence of stress maxima in finite element computations, Comm. Engrg. Numer. Methods 10 (1994) 683–697.
[13] I. Babuška and A. Miller, The post processing approach in the finite element method, Part 1: Calculation of displacements, stresses and other higher derivatives of the displacements, Int. J. Numer. Methods Engrg. 20 (1984) 1085–1109.
[14] K. Izadpanah, Computation of stress components in the P-version of the finite element method, D.Sc. Dissertation, Washington University, 1984.
[15] D. Vasilopoulos, Extraction of two-dimensional stresses on the boundary, GMR Research Publication GMR-7459, August, 1991.
[16] O.C. Zienkiewicz and J.Z. Zhu, Superconvergent patch recovery and a posteriori error estimates, Part 1: The recovery technique, Int. J. Numer. Methods Engrg. 33 (1992) 1331–1364.
[17] I. Babuška and M. Suri, The p- and h-p versions of the finite element method—an overview, Comput. Methods Appl. Mech. Engrg. 80 (1990) 5–26.
[18] J.T. Oden and J.N. Reddy, On dual-complementary variational principles in mathematical physics, Int. J. Engrg. Sci. 12 (1974) 1–29.
[19] J. Penman and J.R. Fraser, Complementary and dual energy finite element principles in magnetostatics, IEEE Trans. Magnetics 18 (1982) 319–324.
[20] Z. Yosibash and B.A. Szabó, Numerical analysis of singularities in two dimensions, Part 1: Computation of eigenpairs, Int. J. Numer. Methods Engrg. 38 (1995) 2055–2082.